

# Computer-Assisted Segmentation of Bacteria in Color Micrographs

Chandan K. Reddy and Frank B. Dazzo, Center for Microbial Ecology, Michigan State University, USA

## BIOGRAPHY

Frank Dazzo is a professor of microbiology at Michigan State University and has conducted microscopy of microorganisms since childhood, producing images widely used in textbooks and websites of microbiology. He currently directs a team of microbiologists, mathematicians and computer scientists to develop CMEIAS software applications in computer-assisted microscopy and image analysis that are designed to improve microscopy-based quantitative approaches for understanding microbial ecology.

## ABSTRACT

We describe a semi-automated method to segment multicolored microbes in digitized color images containing complex, noisy backgrounds. Instead of providing a simple threshold, the system uses an interactive environment whereby one samples multiple pixels to represent the range of color pixels comprising the foreground microbes of interest. The color and spatial distances of these target points are then used to segment the microbes from the confusing background. The new system should have wide applications in digital image analysis of multicolored objects in complex colored images, as is commonplace in studies of in-situ microbial ecology and biomedical imaging.

## KEYWORDS

CMEIAS, color distance, spatial distance, color segmentation, microbial ecology, light microscopy, image analysis

## ACKNOWLEDGMENTS

We thank Feng-I Liu and George Stockman for valuable information and the MSU Center for Microbial Ecology for financial support. This work is part of the master's thesis research of Chandy Reddy, a former graduate student in Computer Science & Engineering at Michigan State University.

## AUTHOR DETAILS

Dr Frank B. Dazzo, 2209 Biomedical & Physical Sciences Bldg., Dept. of Microbiology & Molecular Genetics, Michigan State University, East Lansing, MI 48824, USA.  
Tel: +1 517 355 6463 ext. 1587  
Email: dazzo@msu.edu

*Microscopy and Analysis*, 18 (5): 5-7 (UK), 2004.

## INTRODUCTION

Digital micrographs of micro-organisms in their natural habitats are highly complex, posing major challenges for image processing and advanced analysis [1]. This image complexity is further exacerbated when the microbes have been stained with general colored dyes to increase their contrast and visualization, or with specific chromophores linked to molecular probes that reveal unique cellular components or specific biochemical activities on their surface or interior. Depending on the stain used, the color of the microbes in the digital image can provide useful information on their in-situ biochemical, physiological, ecological and phylogenetic characteristics without the need for their laboratory cultivation. Thus, color images of microbes can contain large amounts of very useful information so long as the foreground objects of interest can be accurately segmented and analyzed. Herein lies the problem: the pixels that comprise the microbial objects of interest typically have a variable color range and therefore these foreground objects cannot be accurately defined using color segmentation routines whose operation is based on isolation of pixels with a single RGB value. The goal of our work summarized here is to develop a system that can semi-automate the segmentation of multicolored foreground microbes so they can be analyzed accurately in digitized color images that also contain complex and usually noisy backgrounds [2,3]. The system described here is a component of CMEIAS (Center for Microbial Ecology Image Analysis System) whose combined purpose is to strengthen microscopy-based approaches for understanding microbial ecology.

## MATERIALS AND METHODS

Bacteria were fixed to slides and stained using the Gram's staining reagents, DAPI, DTAF, FITC-conjugated antibody, RITC-conjugated 16SrDNA oligonucleotide probe, and genetically engineered to express the green fluorescent protein. Constellation microspheres (Molecular Probes, Inc.) were suspended in water and immobilized between a layer of agarose on a microscope slide and the overlying coverslip. Color photomicrographs were acquired on Kodak Ektachrome 160 and 400 transparency slide film using a Zeiss Photomicroscope I equipped for transmitted brightfield and epifluorescence microscopy, and converted to 24-bit RGB digital images using a Microtek Scanmaker 35T-Plus film scanner.

Images of foreground objects (microbes of interest) were segmented using our color recognition system described here, then converted to 8-bit grayscale images and analyzed

using CMEIAS operating in UTHSCSA Image-Tool [4,5]. The results were compared to ground truth data extracted from equivalent images prepared by manual editing.

## RESULTS AND DISCUSSION

Each population of bacteria produced a particular range of color and gradient features. This heterogeneous color range for the pixels of individual microbes in digital images may or may not be noticeable when viewed at 1 zoom, but was very obvious when the image was magnified to view the colors of individual pixels comprising the microbial objects (Figs 1a-e). Since the combinational ratio of the RGB color pixels varied within the individual microbes, a default color range for image processing did not accurately fill the color of each cell for each color stain. The legend to Fig 1 indicates the RGB color ranges of pixels within each bacterium stained with various commonly used fluorochromes, each measured by sampling their individual pixels.

The challenge posed here was to bisect the color image into foreground pixels representing only the microbes of interest segmented from background pixels representing all the other colored microbes and invalid objects and void spaces [6]. This situation necessitated the interactive collection of information from several sample pixels of the target foreground objects so their similarity could be compared to each pixel in the image.

Two comparisons were made: an overall comparison and a nearest-neighbor comparison. First, the image was projected to RGB color space [7] so the distance in color space between each image pixel and the training sample pixels could be measured. The second measurement was the similarity in spatial distance between each image pixel and its nearest sampled point. This second measurement was very important because if the color segmentation algorithm were based just on similarity of the color information, background pixels with color similar to the foreground objects would misclassify as included. To compute this measurement of similarity in spatial distance, a local thresholding was used to compare every individual pixel in the image to its nearest sample point. Every pixel in the image was considered individually and each pixel under consideration at any given time was termed the 'current pixel'. The current pixel had to be compared to the whole set of sample points to avoid excluding foreground objects containing multiple color groups when the sample point of one color group was close to the current pixel but it belonged to another color group. Therefore, a distance-weighted similarity was used to combine both the color

Table 1:  
Results of accuracy testing of our color segmentation system using 16 different color images of bacteria.

| Image Name              | Image Size (pixels) | Pixels Sampled | Foreground Pixels       |            |            |            | Foreground Object Counts |            |             |            |
|-------------------------|---------------------|----------------|-------------------------|------------|------------|------------|--------------------------|------------|-------------|------------|
|                         |                     |                | Ground Truth            | Our Result | Difference | % Accuracy | Ground Truth             | Our Result | Count Error | % Accuracy |
| BacLight green bacteria | 232000              | 36             | 22194                   | 22313      | 119        | 99.5       | 212                      | 212        | 0           | 100        |
| BacLight red bacteria   | 232000              | 62             | 25471                   | 26542      | 1071       | 95.8       | 195                      | 196        | 1           | 99.5       |
| Blood-Clos.Perfringens  | 183150              | 43             | 7682                    | 7397       | 285        | 96.3       | 107                      | 108        | 1           | 99.1       |
| BloodG-rodG+cocci       | 185129              | 28             | 487                     | 423        | 64         | 86.9       | 13                       | 13         | 0           | 100.0      |
| BloodStrepPneumoniae    | 137054              | 45             | 1529                    | 1352       | 177        | 88.4       | 59                       | 61         | 2           | 96.6       |
| Blood-Strept.Pyogenes   | 141321              | 27             | 654                     | 592        | 62         | 90.5       | 40                       | 38         | 2           | 95.0       |
| Constellation-dapi-1    | 133172              | 23             | 3245                    | 2907       | 338        | 89.6       | 7                        | 7          | 0           | 100.0      |
| Constellation-fitc-1    | 111720              | 21             | 3275                    | 2963       | 312        | 90.5       | 12                       | 16         | 4           | 66.7       |
| Dapi-k bacteria         | 97869               | 47             | 4126                    | 3884       | 242        | 94.1       | 16                       | 16         | 0           | 100.0      |
| E11Fitc-antiE11-a       | 579361              | 76             | 35183                   | 33747      | 1436       | 95.9       | 31                       | 30         | 1           | 96.8       |
| E11-Fitc-antiE11-b      | 42680               | 36             | 2517                    | 2726       | 209        | 91.7       | 58                       | 60         | 2           | 96.6       |
| Nasopharynx Microflora  | 461660              | 39             | 4376                    | 4280       | 96         | 97.8       | 70                       | 70         | 0           | 100.0      |
| RitcFISHdapi-blue       | 124620              | 15             | 2163                    | 1985       | 178        | 91.8       | 5                        | 5          | 0           | 100.0      |
| RitcFISHdapi-red        | 124620              | 31             | 7872                    | 7845       | 27         | 99.7       | 12                       | 12         | 0           | 100.0      |
| RitcFISH-I              | 173720              | 9              | 5924                    | 5558       | 366        | 93.8       | 18                       | 18         | 0           | 100.0      |
| Wur20-Rhizobacteria     | 233530              | 23             | 2322                    | 2226       | 96         | 95.9       | 44                       | 43         | 1           | 97.7       |
|                         |                     |                | Average % Accuracy 93.6 |            |            |            | Average % Accuracy 96.7  |            |             |            |

and the spatial distances. This adaptive neighborhood comparison worked very well for most test images that had noisy and uneven color distributions. However, this comparison encountered problems when attempting to segment foreground objects representing several different color groups. In such cases, the nearest neighbor comparison could only belong to one of those color groups. Thus multiple segmented images must be prepared from this primary image, one for each different color group that the user wants to segment, as illustrated in Fig 2. It was very possible that the current pixel belongs to another color group, which was not the same one as its nearest neighbor. In this case, we needed to use the overall comparison in the distance formula. High efficiency of the prototype system was clearly illustrated even when the input image had varying colors of background pixels that were similar to the foreground. Depending on how many target groups there were in the application, we adjusted the importance of the nearest neighbor comparison and overall comparison by modifying the weight of each term (see [9]).

The selection of sample training points was an interactive input that required great care since it would significantly affect the quality of the results. Our method required knowledge provided by carefully sampled training points whose color and spatial position were the only information describing the desired target group. These computed values must accurately represent the range of features of the target group in order for our method to produce the

optimal color segmentation result. Figure 2 illustrates the application of our color recognition system.

To evaluate the performance of our system, the results of color segmentation was compared to ground-truth data accurately representing the target objects [8]. Since no absolute ground-truth data could be produced directly without human intervention, they had to be acquired using images that had been edited manually. Two different types of error were measured: false alarm (non-object pixels treated as foreground objects) and false dismissal (foreground object pixels treated as non-object background) [9]. We performed a pixel-by-pixel comparison of each pixel in the test result images to the ground truth images to determine if each pixel was classified correctly. The measure we used for this comparison was not just the total number of pixels. Instead, if the segmentation result produced objects of the same size but with a wrong boundary, this measurement of area reflected an incorrect shape or boundary. The errors were measured as the number of incorrectly classified pixels (area) divided by the total pixels of the image and reported as the total percent of error in size. The results are summarized in Table 1.

The color segmentation system provided very good results in defining the area of the foreground objects since the false-alarm and false-dismissal errors were relatively low, yielding an overall average percent accuracy of 93.6% using our microbial test images (Table

1). The major source of the false-alarm error came from the manually drawn boundary between touching cells. The false-dismissal error arose primarily because the boundary between the microbial cell itself and the fluorescent halo surrounding it (considered background) in fluorescent micrographs was often indistinct (Fig 1e), and therefore the system sometimes selected a different boundary than the one defined by human intervention to produce the ground-truth data, even though the shape of the foreground object remained similar in both data outputs. As anticipated, the results were better when the boundary separating foreground/background pixels was easily distinguishable. Applying a minimum/maximum object filter and dilation/erosion image processing routines can help to reduce this type of false-dismissal error. The system's ability to produce derived images from which the colored foreground microbes of interest could be accurately detected and counted automatically was also very good, with an overall average accuracy of 96.7% for the test images (Table 1).

The weighted similarity measurement of our proposed system provided the flexibility to adapt to many different color groups for the segmentation process. A sufficient number of good sample points must interactively be picked that can fully represent the target color group to achieve the best results, and doing this task while viewing the cells in a zoom mode can be helpful. Successful segmentation of color images with complex backgrounds

also requires that training sample points be picked in various regions of interest to indicate ambiguous regions whose color is not well defined. The time spent will depend on the image size and number of sampled points needed to represent the target group, but it will always be quicker than the alternative of manual editing alone.

## CONCLUSIONS

This article describes our computer vision-based semi-automated method to segment microbes of interest in complex digitized color micrographs for quantitative image analysis. Experimental testing indicated that the system performed with an overall accuracy of 96.7% in finding the foreground objects of interest, and 93.6% in defining their two-dimensional projected area. By using the weighted similarity measurement and adaptive neighborhood scheme, our proposed system provided the flexibility to adapt to several different color groups for the segmentation process, even with complex backgrounds. These characteristics all translate to a reduction in user's time and labor costs required to perform this essential image-editing step, hence facilitating the whole process of digital image analysis. As with all applications of digital image analysis, the original color images of the microorganisms must be of high quality as a prerequisite.

We anticipate that the operating principles of this segmentation tool will create new opportunities for quantitative image analysis of any foreground objects of interest differentiated by color in digital RGB images. Examples of microbiological applications include quantification of certain microbial pathogens in Gram-stained clinical specimens, detection and autecological studies of selected microbes using immunofluorescence microscopy, phylogenetic analysis of microbial abundance and diversity in natural communities by fluorescent in-situ hybridization using fluorescently labeled 16SrDNA oligonucleotide molecular probes, and in-situ spatial distribution analysis of cell-associated metabolic activities in microbial biofilms. Our first application of this semi-automated color segmentation system was to produce segmented color images for analysis of the in-situ spatial distribution of genetically-engineered red fluorescent bacteria that provide a source of quorum sensing cell-to-cell communication molecules during their colonization of plant roots [10]. When fully developed, the software application described here will be available at: <http://cme.msu.edu/cmeias>

## REFERENCES

1. Wilkinson, M. H. and Schut F. Digital Image Analysis of Microbes: Imaging, Morphometry, Fluorometry, and Motility Techniques and Applications. John Wiley & Sons, UK, 1998.
2. Fuh C. S. et al. Hierarchical color image region segmentation for content-based image retrieval system. IEEE Transactions on Image Processing 9, 156-162, 2000.
3. Zhou J. et al. Multiresolution filtering with application to image segmentation. Mathematical Computer Modeling 24, 177-195, 1996.
4. Liu, J. et al. CMEIAS: a computer-aided system for the image analysis of bacterial morphotypes in microbial communities.

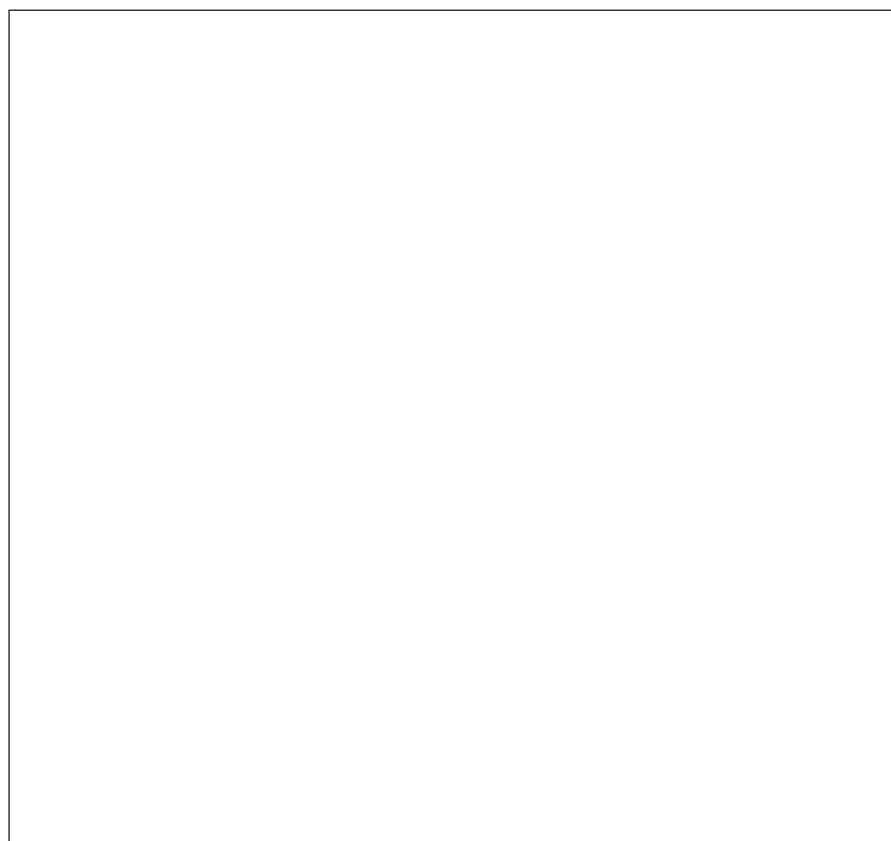


Figure 1:

Bacterial cells in digital color of bacterial cells. Pixels that comprise the bacterial objects contain a complexity of RGB values revealed by viewing at high zoom. The color stains and their corresponding RGB ranges are: (a) rhodamine r124-r217, g0, b1-b8; (b) DAPI, r1-74, g49-g191, b157-b255; (c) crystal violet, r62-r157, g0, b167-b227; (d) DTAF, r116-r179, g166-g246, b167-b227; (e) FITC, r92-r118, g198-g255, b0. Scale bar = 0.5  $\mu$ m.

- Microbial Ecology 41, 173-194, 2001 and 42, 215, 2001. <http://cme.msu.edu/cmeias>
5. Wilcox C. D. et al. UTHSCSA ImageTool Ver. 1.27, Univ. Texas Health Science Center, San Antonio, TX. <http://ddstdx.uthscsa.edu/dig/itdesc.html>
6. Dubuisson M. P. et al. Segmentation and classification of bacterial culture images. J. Microbiol. Methods 19, 279-295, 1994.
7. Wyszecki, G. and Styles, W. S. Color Science: Concepts and Methods, Quantitative Data and Formulae, 2nd Ed., John Wiley & Sons, Inc., NY, 1982.
8. Sieracki M. E. et al. Evaluation of automated threshold selection methods for accurately sizing microscopic fluorescent cells by image analysis. Appl. Environ. Microbiol. 55, 2762-2772, 1989.
9. Ready C. K. et al. Semi-automated segmentation of microbes in color images. Proc. SPIE-IS&T Electronic Imaging, SPIE Vol. 5008, pp.548-559, Santa Clara, CA, 2003.
10. Gantner S. et al. In situ spatial scale of calling distances in bacterial cell communication. Submitted 2004.

©2004 John Wiley & Sons Ltd

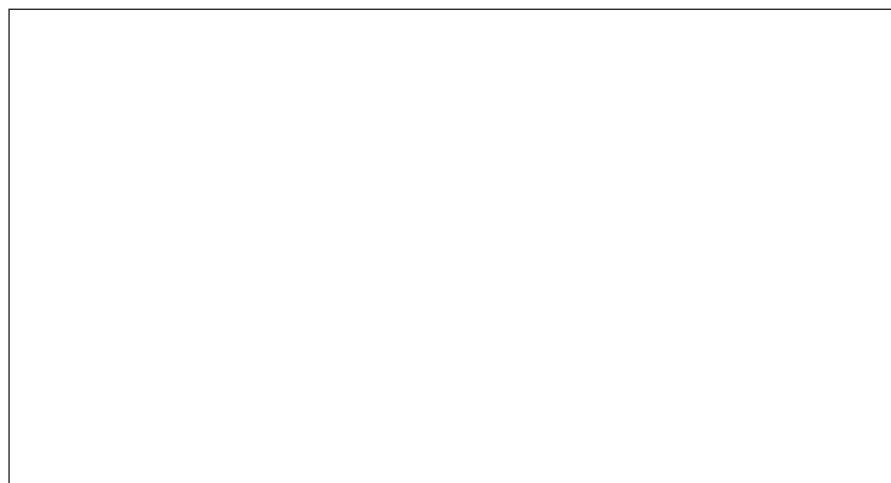


Figure 2:

Color segmentation of multicolored bacteria in a single composite RGB image using our proposed system. Bacteria (left to right) were stained with RITC, FITC, DAPI, and the Gram's staining reagents. The gray arrows point to the region of the derived image containing only the corresponding foreground objects of interest in a noise-free background.